An Optimization of a Circular Antenna Array for On-Body Communication

Hanne Herssens, Arno Thielens
Department of Information Technology, Ghent University - imec, 9000 Ghent, Belgium, hanne.herssens@ugent.be

***Abstract*—A non-uniform circular array wrapped around the waist is proposed for on-body communication with uniform on-body coverage at 5 GHz. To investigate the feasibility of such an array, we determined the path loss between such an array and on-body nodes using simulations and measurements on a cylindrical phantom and a real person. The number of array elements is varied to establish that uniform on-body coverage can be achieved. The best combination of array elements on a real person in terms of uniform on-body coverage is found with 4 elements distributed along the array, i.e., they were not found on one side of the body. A higher number of elements leads to a higher potential on-body gain, but also to a decrease in uniformity of the on-body coverage. These results are important for emerging WBAN applications that require uniform coverage of a large number of nodes spread over the human body.**

***Index Terms*—Circular antenna array, distributed antenna array, on-body communication, wireless body area network**

I. Introduction

Wireless body area networks (WBANs) are collections of on-body nodes that can monitor body-related information, e.g., the health of a patient, the performance of an athlete, or the safety of workers [1], [2]. These on-body nodes collect data and transmit these data to other nodes in the WBAN. This occurs through so-called on-body communication, which is the focus of this paper. These wireless transmissions happen using on-body antennas. The on-body nodes need to be wearable and therefore the antennas should be compact. Additionally, the antenna design needs to be optimized for the on-body environment, since the human body will affect the antenna parameters [3], [4].

Single on-body antennas can suffer from high propagation losses caused by the human body [5], [6]. To overcome this problem, antenna arrays can be used to increase the gain. In an array, a higher gain can be obtained by combining multiple antenna elements. However, the wearability of the array will place a limit on the number of elements that can be used. In on-body communication, on-body nodes on opposite sides of the body will be shielded from each other. Additional propagation losses can occur due to human body shadowing [7]. A distributed array, where the elements are spread over the body, could provide a solution to this issue. In theory, it is possible to design this type of array in such a way that there is always at least one other antenna in line-of-sight (LOS) conditions with every on-body node present in a WBAN.

A circular antenna array wrapped around, e.g., the waist, is an example of such a distributed array. This type of array has not been studied extensively, despite its potential. In [8], the path loss on the body at $5.8\,\mathrm{GHz}$ of a circular array is investigated. This array is wrapped around the arm and consists of 4 equally spaced patch antennas for which the goal was to obtain an omnidirectional radiation pattern. When this array is wrapped around an arm, the opposite side of the body will still be shielded, as observed by the authors of [8]. In [9], a circular antenna array is wrapped around the human trunk for off-body communication at $5\,\mathrm{GHz}$. Again, the goal was to achieve an omnidirectional radiation pattern. Other examples of circular arrays are found in [7], [10], [11]. In the previous papers, the antenna elements were excited with uniform amplitude and phase. Exciting the antenna elements by different phases could increase the radiation in a desired direction, which could improve on-body or off-body links in a WBAN. Additionally, these prior studies have not investigated a non-uniform circular array, where the antenna elements are not equally spaced in the circular array.

Therefore, the goal of this paper is to optimize the performance of a non-uniform circular array (NUCA) wrapped around the waist for on-body communication in terms of uniform on-body coverage. This is done by varying the number of elements in the array and see how this influences the on-body path loss and if uniform body coverage can be achieved. Measurements and simulations are performed on a cylindrical phantom and on a real person and the results are compared.

II. Circular Antenna Array

The measurements and simulations were performed using patch antennas operating at $4.56\,\mathrm{GHz}$ (Fig. 1a). The antenna is fabricated with copper on FR-4. The FR-4 substrate has a height of $1.55\,\mathrm{mm}$. The measurements were performed using a vector network analyzer (VNA, ZNB20, Rohde & Schwarz) over a frequency band from $4.36\,\mathrm{GHz}$ to $4.76\,\mathrm{GHz}$. The frequency sweep consists of 401 equidistant steps and is repeated 50 times. The simulations were performed using the Finite-Difference Time-Domain (FDTD) method in Sim4Life (ZMT, Zürich, Switzerland), where PEC material was used for the copper and dielectric constants $\epsilon_r = 4.9$ and $\sigma = 0.0038\,\mathrm{S/m}$ (Sim4Life database) for the FR-4 substrate. The measured reflection coefficient in free space is shown in Fig. 1b. The patch antenna has a bandwidth of $130\,\mathrm{MHz}$.

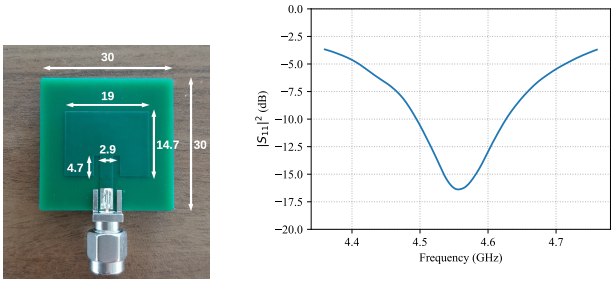

(a) (b)

Fig. 1. (a) Fabricated patch antenna with dimensions in mm. The height of the substrate is 1.55 mm. (b) Measured reflection coefficient in free space.

These patch antennas will be placed in a circular array as shown in Fig. 2. The array will be a virtual array. This means that a single antenna element will be moved to each array position and that the full array will be obtained in a post-processing step. This is only valid when the mutual coupling between two elements in the array is minimal. Our measurements show that the mutual coupling between array elements 1 and 2 on a cylinder (Fig. 3a) is $< -40\,\mathrm{dB}$.

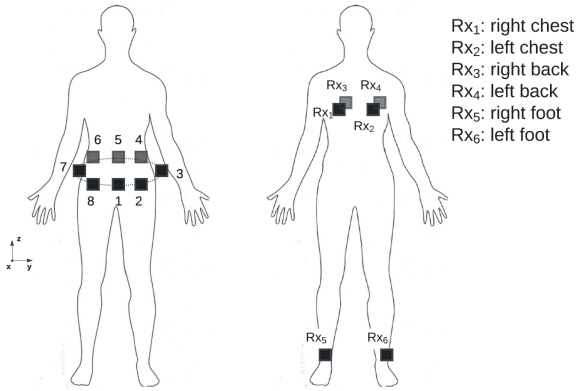

(a) (b)

Fig. 2. (a) Circular antenna array on the body. (b) Receiver (Rx) locations on the body. The rectangles represent the antennas. The transparent rectangles are located at the back of the body.

III. Quantities

This section introduces the quantities that are used in this paper for studying the performance of the array in terms of uniform on-body coverage.

The measured S_{21} between the array and a receiver (Rx) is used as a measure for the path loss. When equal gain transmission (EGT) is applied at the Rx locations [12], the EGT-precoded S_{21} can be written as:

$$S_{21,\,EGT}(k) = \frac{1}{\sqrt{m}} \sum_{l=1}^{m} S_{21,\,kl} \exp\left(-j * arg(S_{21,\,kl})\right) \quad (1)$$

with m the number of array elements and k the Rx location.

The normal component of the electric field at the Rx location is used as a proxy for the path loss in the simulations, since using S_{21} would lead to a large number of simulations. A higher obtained electric field at the Rx indicates a lower path loss. The normal component of the EGT-precoded electric field is as follows:

$$E_{n,EGT}(k) = \frac{1}{\sqrt{m}} \mathbf{n} \cdot \sum_{l=1}^{m} \mathbf{E}_{kl} \exp\left(-j * arg(\mathbf{n} \cdot \mathbf{E}_{kl})\right) \quad (2)$$

with m the number of array elements, k the Rx location and $\mathbf{n}$ the normal vector on the surface at location k.

In this paper, the uniformity of the on-body coverage is defined by looking at the range between the 5th and 95th percentiles of the measured $|S_{21}|^2_{EGT}$ or the simulated $|E_n|^2_{EGT}$ between an array of m elements and the potential Rx locations. The uniformity in dB is defined as $U = -(p_{95} - p_5)$. The uniformity is maximal when the range $p_{95} - p_5$ is minimal.

To determine the best combination for a certain number of array elements m in terms of uniform on-body coverage, a figure of merit (FOM) is defined by looking at the path loss and the uniformity:

$$FOM\ (\mathrm{dB}) = p_{50} + U \quad (3)$$

The best combination will have minimal path loss (high p_{50}) and maximal uniformity of the on-body coverage (high U).

IV. Path Loss on Cylindrical Phantom

A. Measurements

The on-body path loss is measured on a PVC cylinder filled with tap water. The radius of the cylinder is $r = 125\,\mathrm{mm}$ and the thickness of the PVC material is $5\,\mathrm{mm}$. The set-up is shown in Fig. 3. The cylindrical phantom can be used to study the uniform on-body coverage in the azimuthal direction due to its symmetry. The S_{21}-parameters between the array elements and a Rx (patch antenna) are measured using a VNA. S_{21} is averaged over 10 measurements to lower the noise. The Rx antenna is moved, while the transmitter (Tx) antenna is kept at the same location (virtual array) for each element. S_{21} on the cylinder is obtained by using the symmetry of the cylinder. S_{21} only needs to be measured for $\phi = 0$ to $\phi = \pi$. S_{21} for $\phi > \pi$ is obtained by rotating the results in post-processing. The Rx antenna is placed $10\,\mathrm{cm}$ above the Tx antenna for $\phi = 0..\pi$ with $d\phi = 2\pi/20$. In this set-up, 20 possible Tx positions are considered (Fig. 3a). The number of elements present in the array will be varied from 1 to 20, and all possible combinations for a certain number of elements will be considered.

Fig. 4a shows the median value of the measured $|S_{21}|^2_{EGT}$ as a function of the number of antenna elements m for all possible combinations of m array elements and Rx location on the cylinder. The brackets indicate the 5th and 95th percentiles. Fig. 4a shows that higher fields are found for increasing m. The median value increases from $-68\,\mathrm{dB}$ to $-32\,\mathrm{dB}$ for $m = 1$ to $m = 20$. The uniformity increases from $-52\,\mathrm{dB}$ to $0\,\mathrm{dB}$ from $m = 1$ to $m = 20$. Therefore, the on-body coverage will be more uniform for increasing m.

Fig. 4b shows the median value of $|S_{21}|^2_{EGT}$ over the Rx locations for the best combination of m elements in the

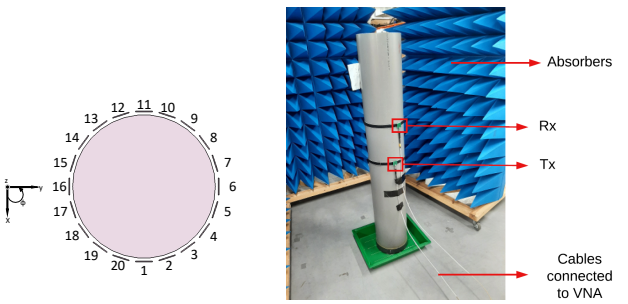

(a) (b)

Fig. 3. Cylindrical phantom with radius $r = 125\,\mathrm{mm}$. (a) Top view. The rectangles represent the antennas. (b) Measurement set-up.

array determined by (3). The brackets indicate the 5th and 95th percentiles. With 10 elements, the uniformity of the on-body coverage is already maximal ($U = -0.5\,\mathrm{dB}$). However, increasing the number of elements can still lead to higher fields, i.e., the median increases from $-35\,\mathrm{dB}$ to $-32\,\mathrm{dB}$ from $m = 10$ to $m = 20$. The uniform on-body coverage will benefit from more symmetry. The best combinations for which m is a divisor of 20, i.e., $m = 1$, 2, 4, 5, 10, and 20, are the combinations where the m elements are equally spaced in the array, i.e., a uniform circular array (UCA) is formed.

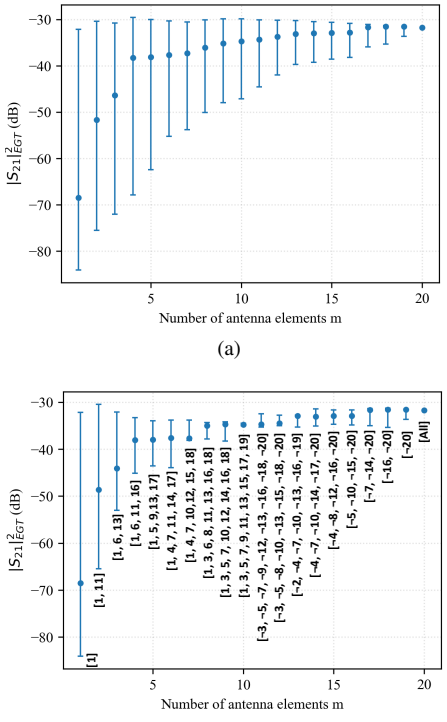

(a)

(b)

Fig. 4. (a) The median value of $|S_{21}|^2_{EGT}$ as a function of the number of antenna elements m for all possible combinations of m array elements and Rx location on the cylinder. The brackets indicate the 5th and 95th percentiles. (b) The median value of $|S_{21}|^2_{EGT}$ over the possible Rx locations for the best combination of m elements in the array. The brackets indicate the 5th and 95th percentiles. The labels indicate the element numbers of the best combination in Fig. 3a. The symbol ¬ indicates that the element is not used.

B. Simulations

The measurements were also compared with simulations. The same PVC cylinder ($\epsilon_r = 3$, $\sigma = 0.006\,\mathrm{S/m}$) filled with water is modelled in Sim4Life with thickness $5\,\mathrm{mm}$ and radius $125\,\mathrm{mm}$. The same Rx locations of the measurements are considered.

Fig. 5a plots the median value of $|E_n|^2_{EGT}$ as a function of the number of antenna elements m for all possible combinations of m array elements and Rx location on the cylinder with the total transmitted power normalized to $1\,\mathrm{W}$. The brackets indicate the 5th and 95th percentiles. Fig. 5a shows that the median value increases from $11\,\mathrm{dB}$ to $36\,\mathrm{dB}$ from $m = 1$ to $m = 20$. The uniformity U increases from $-44\,\mathrm{dB}$ to $0\,\mathrm{dB}$ for $m = 1$ to $m = 20$. The simulation results agree with the measurement results, i.e., higher fields and a better uniform on-body coverage is found for an increasing number of elements m in the array.

Fig. 5b plots the median value of $|E_n|^2_{EGT}$ over the Rx locations for the best combination of m elements in the array determined by (3). The brackets indicate the 5th and 95th percentiles. $m = 10$ shows a uniform on-body coverage ($U = -1.4\,\mathrm{dB}$), but increasing the number of elements m will increase the fields. This was also the case with the measurements.

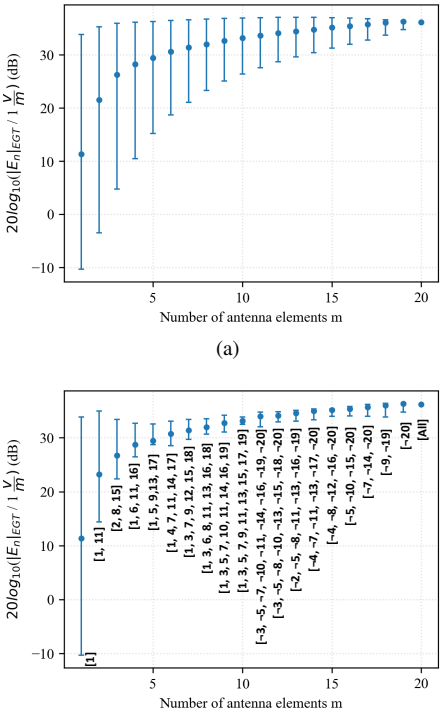

(a)

(b)

Fig. 5. (a) The median value of $|E_n|^2_{EGT}$ as a function of the number of antenna elements m for all possible combinations of m array elements and Rx location on the cylinder with the total transmitted power normalized to $1\,\mathrm{W}$. The brackets indicate the 5th and 95th percentiles. (b) The median value of $|E_n|^2_{EGT}$ over the Rx locations for the best combination of m elements in the array with the total transmitted power normalized to $1\,\mathrm{W}$. The brackets indicate the 5th and 95th percentiles. The labels indicate the element numbers of the best combination in Fig. 3a. The symbol ¬ indicates that the element is not used.

V. On-Body Path Loss

A. Measurements

The on-body path loss between an array element and a Rx antenna is measured with a VNA on a male subject with height 1.91 m. The number of array elements will be varied from 1 to 8 and S_{21} is measured at 6 Rx locations. All possible combinations of m elements in the array will be considered. The Rx locations and the possible array element locations are illustrated in Fig. 2. The average of 50 S_{21}-values is taken to lower the noise.

Fig. 6a shows the median value of the measured $|S_{21}|^2_{EGT}$ as a function of the number of antenna elements m for all possible combinations of m array elements and Rx location on the body. The brackets indicate the 5th and 95th percentiles. Higher fields are found for an increasing number of elements m. The median increases from $-64\,\mathrm{dB}$ to $-48\,\mathrm{dB}$ for $m = 1$ to $m = 8$. The uniformity U increases from $-43\,\mathrm{dB}$ to $-17\,\mathrm{dB}$ for $m = 1$ to $m = 8$. More array elements will lead to a more uniform on-body coverage for the set of Rx locations shown in Fig. 2b.

Fig. 6b shows the median value of $|S_{21}|^2_{EGT}$ over the possible Rx locations for the best combination of m elements in the array determined by (3). The brackets indicate the 5th and 95th percentiles. $m = 1$ shows the highest uniformity ($U = -12\,\mathrm{dB}$) compared to the other number of elements. However, Fig. 6a also shows that fields for $m = 1$ are much lower ($p_{50} = -65\,\mathrm{dB}$) compared to the fields for the other values of m ($p_{50} > -55\,\mathrm{dB}$). When $m = 1$ the best combination is found for array element 7 in Fig. 2a. This element will lead to comparable values of S_{21} for the Rx locations on the back and on the front of the body, i.e., the on-body coverage will be uniform, but these values will be low. A higher median value can be found for other elements, but these elements will lead to high values of S_{21} on the same side of the array element and low values on the other side. Therefore, the on-body coverage will be less uniform. Disregarding the case $m = 1$, the most uniform on-body coverage is found for $m = 4$ ($U = -12.3\,\mathrm{dB}$) for the combination of array elements 2, 4, 7 and 8 with a median value of $p_{50} = -51\,\mathrm{dB}$. This combination distributes the array elements along the array, i.e., they are not found on one side of the body. The UCA with 4 elements, i.e., elements 1, 3, 5 and 7, leads to a comparable median value $p_{50} = -51.3\,\mathrm{dB}$, but the on-body coverage decreases to $U = -18\,\mathrm{dB}$. Higher fields are found for $m = 8$ ($p_{50} = -48\,\mathrm{dB}$), but the on-body coverage will be less uniform ($U = -17\,\mathrm{dB}$).

B. Simulations

The measurement results were compared with simulations. The simulations were performed using the ViP Duke heterogeneous phantom [13]. The phantom consists of 305 different tissues with dielectric parameters found in [14]. The phantom is discretized with a grid step of 2 mm in each direction.

Fig. 7a shows the median value of the simulated $|E_n|^2_{EGT}$ as a function of the number of antenna elements m for all possible combinations of m array elements and Rx location on the body. The brackets indicate the 5th and 95th percentiles. Increasing the number of elements m leads to higher fields. The median value increases from $1\,\mathrm{dB}$ to $26\,\mathrm{dB}$ for $m = 1$ to $m = 8$. More antenna elements lead to a more uniform on-body coverage, i.e., U increases from $-45\,\mathrm{dB}$ to $-18\,\mathrm{dB}$ for $m = 1$ to $m = 8$.

Fig. 7b shows the median value of $|E_n|^2_{EGT}$ over the possible Rx locations for the best combination of m elements in the array determined by (3). The brackets indicate the 5th and 95th percentiles. The most uniform on-body coverage is found for $m = 4$ with $U = -15.3\,\mathrm{dB}$ and $p_{50} = 22\,\mathrm{dB}$ for the combinations of array elements 2, 3, 5 and 8. Again, the best combination is found for 4 elements distributed along the array. The UCA consisting of 4 elements leads to a comparable median value $p_{50} = 22.2\,\mathrm{dB}$, but the uniformity decreases to $U = -21\,\mathrm{dB}$. Higher fields are found for $m = 8$, but the on-body coverage is less uniform.

The simulation results show a median value close to the 95th percentile. This is explained by the fact that 4 out of 6 Rx locations are found at the front of the body (Fig. 2b). Therefore, the best combination will favor the array elements at the front of the body. This can be seen by the best combination of array elements for $m = 4$, i.e., 2 of the elements are

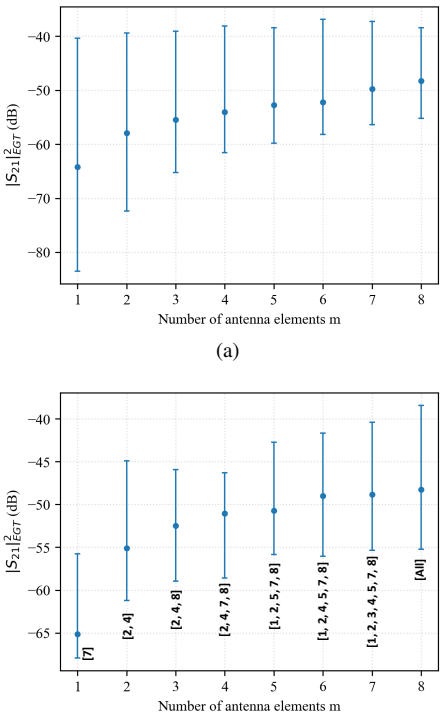

Fig. 6. (a) The median value of $|S_{21}|^2_{EGT}$ as a function of the number of antenna elements m for all possible combinations of m array elements and Rx location on the body. The brackets indicate the 5th and 95th percentiles. (b) The median value of $|S_{21}|^2_{EGT}$ over the possible Rx locations for the best combination of m elements in the array. The brackets indicate the 5th and 95th percentiles. The labels indicate the element numbers of the best combination in Fig. 2a.

found at the front of the body compared to 1 element at the back. This was also the case with the measurements.

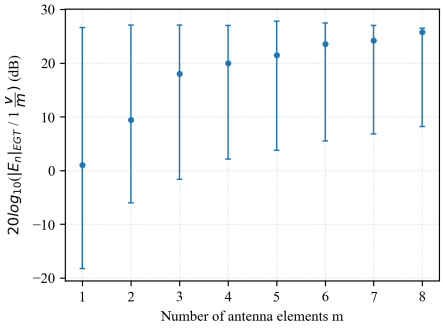

(a)

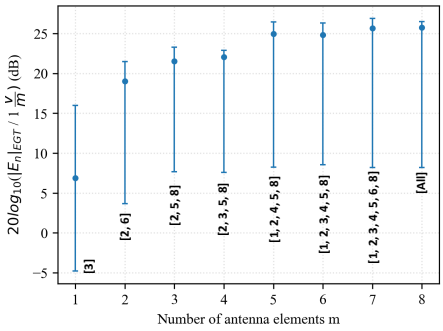

(b)

Fig. 7. (a) The median value of $|E_n|^2_{EGT}$ as a function of the number of antenna elements m for all possible combinations of m array elements and Rx location on the body with the total transmitted power normalized to 1 W. The brackets indicate the 5th and 95th percentiles. (b) The median value of $|E_n|^2_{EGT}$ over the possible Rx locations for the best combination of m elements in the array with the total transmitted power normalized to 1 W. The brackets indicate the 5th and 95th percentiles. The labels indicate the element numbers of the best combination in Fig. 2a.

VI. Conclusion

A non-uniform circular antenna array wrapped around the waist is optimized for on-body communication. The goal of this array is to achieve uniform on-body coverage. The path loss on a cylindrical phantom filled with tap water and on a real person is measured and simulated and the results were compared. The best combination for a certain number of array elements is found when the array elements are distributed (almost) uniformly along the array. The simulation and measurement results agree well with each other. For the cylindrical phantom, the best configuration was obtained for 10 antennas spread over the cylinder's circumference. This resulted in a median on-body gain of $-35\,\mathrm{dB}$ under EGT with a spread on this median characterized by $p_{95}-p_5 = 0.5\,\mathrm{dB}$ for the measurements. The best combination of array elements in terms of uniform on-body coverage on a real person consists of 4 elements for both the simulations and the measurements. These elements were distributed along the array, which was also the case with the cylindrical phantom. The measurements for the best combination resulted in a median on-body gain of $-51\,\mathrm{dB}$ with a spread on this median characterized by $p_{95}-p_5 = 12.3\,\mathrm{dB}$. More elements in the array lead to higher fields, but the on-body coverage becomes less uniform. The uniform on-body coverage will benefit from a distributed array, when the Rx locations are spread over the body. Therefore, WBANs for which the locations of the on-body sensors are spread over the body or not initially known, will benefit from this type of array.

Acknowledgment

Arno Thielens is a postdoctoral fellow of the Research Foundation Flanders (FWO) under grant agreement no. 1283921N.

References

[1] M. Ghamari *et al.*, "A Survey on Wireless Body Area Networks for eHealthcare Systems in Residential Environments," *Sensors*, vol. 16, no. 6, 2016.

[2] Q. Liu, K. G. Mkongwa, and C. Zhang, "Performance issues in wireless body area networks for the healthcare application: a survey and future prospects," *SN Applied Sciences*, vol. 3, no. 2, pp. 1–19, 2021.

[3] P. S. Hall *et al.*, "Antennas and propagation for on-body communication systems," *IEEE Antennas and Propag. Magazine*, vol. 49, no. 3, pp. 41–58, 2007.

[4] L. Roelens, W. Joseph, E. Reusens, G. Vermeeren, and L. Martens, "Characterization of Scattering Parameters Near a Flat Phantom for Wireless Body Area Networks," *IEEE Trans. on Electromagn. Compat.*, vol. 50, no. 1, pp. 185–193, 2008.

[5] E. Reusens *et al.*, "Characterization of On-Body Communication Channel and Energy Efficient Topology Design for Wireless Body Area Networks," *IEEE Trans. on Inf. Techn. in BioMed.*, vol. 13, no. 6, pp. 933–945, 2009.

[6] A. Thielens *et al.*, "A Comparative Study of On-Body Radio-Frequency Links in the 420 MHz–2.4 GHz Range," *Sensors*, vol. 18, no. 12, 2018.

[7] L. Januszkiewicz, "The analysis of textile antenna array radiation pattern," in *18th Int. Conf. on Microw., Radar and Wireless Commun.*, 2010, pp. 1–4.

[8] C.-X. Mao, D. Vital, D. H. Werner, Y. Wu, and S. Bhardwaj, "Dual-Polarized Embroidered Textile Armband Antenna Array With Omnidirectional Radiation for On-/Off-Body Wearable Applications," *IEEE Trans. on Antennas and Propag.*, vol. 68, no. 4, pp. 2575–2584, 2020.

[9] Y. Li, L. Yang, M. Gao, X. Zhao, and X. Zhang, "A study of a one-turn circular patch antenna array and the influence of the human body on the characteristics of the antenna," *Ad Hoc Net.*, vol. 99, p. 102059, 2020.

[10] H. Yang, X. Liu, and Y. Fan, "Design of Broadband Circularly Polarized All-Textile Antenna and Its Conformal Array for Wearable Devices," *IEEE Trans. on Antennas and Propag.*, vol. 70, no. 1, pp. 209–220, 2022.

[11] Y. Li and M. Zhang, "Study on a Cylindrical Sensor Network for Intelligent Health Monitoring and Prognosis," *IEEE Access*, vol. 6, pp. 69 195–69 202, 2018.

[12] S. Saunders and A. Aragón-Zavala, *Antennas and Propagation for Wireless Communication Systems*. Wiley, 2007.

[13] M.-C. Gosselin *et al.*, "Development of a new generation of high-resolution anatomical models for medical device evaluation: the Virtual Population 3.0," *Phys. in Med. & Biol.*, vol. 59, no. 18, p. 5287, 2014.

[14] P. Hasgall *et al.*, "IT'IS Database for thermal and electromagnetic parameters of biological tissues, Version 4.0," *IT'IS*, 2018.